



Kinetic study of benzyl sulfamide synthesis by thermolysis of *N*-(benzyl)-*N'*-(*tert*-butoxycarbonyl) sulfamide

Luciana Gavernet ^a, Maria Luisa Villalba ^a, Luis Bruno Blanch ^a and Ileana Daniela Lick ^{b,*}

^a Medicinal Chemistry, Department of Biological Sciences, Faculty of Exact Sciences, National University of La Plata, La Plata, B1900BJW, Argentina

^b Department of Chemistry, Faculty of Exact Sciences, National University of La Plata, CINDECA (CCT-La Plata-CONICET-UNLP), La Plata, B1900BJW, Argentina

*Corresponding author at: Department of Chemistry, Faculty of Exact Sciences, National University of La Plata, CINDECA (CCT-La Plata-CONICET-UNLP), La Plata, B1900BJW, Argentina. Tel.: +54.221.4211353; fax: +54.221.4211353. E-mail address: lick@quimica.unlp.edu.ar (I.D. Lick).

ARTICLE INFORMATION

Received: 17 December 2012

Accepted: 05 January 2012

Online: 31 March 2013

KEYWORDS

Sulfamides

Kinetic study

Benzylsulfamide

Model-free method

Thermolysis reaction

Isoconversional method

ABSTRACT

In this investigation, a kinetic study of the thermolysis of *N*-(benzyl)-*N'*-(*tert*-butoxycarbonyl) sulfamide to yield benzylsulfamide in an efficient manner was performed. The thermolysis reaction was monitored in helium flow by thermogravimetry at different heating rates between 0.2 and 10 °C/min. The activation energy value was obtained from the Kissinger-Akahira-Sunose isoconversional method and theoretical calculations (from Transition State Theory). The reaction model of the process was studied by means of the master-plot method. Results obtained from experiments of thermolysis performed under the melting point temperature of *N*-(benzyl)-*N'*-(*tert*-butoxycarbonyl) sulfamide fit with an Avrami-Erofeev model whereas data found for experiments at higher temperatures fit with first order model. Isothermal experiments were simulated at 115, 120 and 130 °C using the model-free method, employing only the activation energy value.

1. Introduction

Sulfamides and their derivatives have proven to be promising structures with biological activity. Compounds bearing this functionality have been tested as HIV protease inhibitors [1,2], agonists of the 5-HT_{1D} receptor [3], active components in epinephrine analogues [4], non-hydrolyzable components of peptide-mimetics [5] and carbonic anhydrase inhibitors [6-10]. Particularly, it has been demonstrated that benzylsulfamide presents an interesting antiepileptic profile: it can be classified as class 1 candidate according to the standard anticonvulsant screening protocols [11]. Results obtained in the biological stage for benzylsulfamide and other structurally related compounds encouraged us to improve the synthetic strategies for the preparation of sulfamides.

Traditionally, benzylsulfamide was obtained through the preparation of the *N*-*tert*-butoxycarbonyl sulfamide derivative, named *N*-(benzyl)-*N'*-(*tert*-butoxycarbonyl) sulfamide (Compound **1**, Scheme 1), followed by acidic hydrolysis. This intermediate was prepared from chlorosulfonyl isocyanate, *tert*-butanol, and the benzylamine in presence of triethylamine (TEA). The *tert*butoxycarbonyl group was then removed via trifluoroacetic acid (TFA), (Scheme 1).

Recently, an alternative synthetic method was proposed to replace the hydrolysis reaction of the precursor **1** by its thermolysis degradation to yield benzylsulfamide [12]. This new method not only improved the degree of conversion and diminished the reaction time relative to the traditional hydrolysis, but also reduced the generation of waste since it avoided the use of toxic (and/or hazardous) reagents and solvents [12].

The analysis of gaseous by-products produced in the thermolysis reaction supported our suggestion that the decomposition proceeds in a similar route than *N,N*-dialkyl carbamates [12], giving CO₂ and 2-methylpropene as secondary

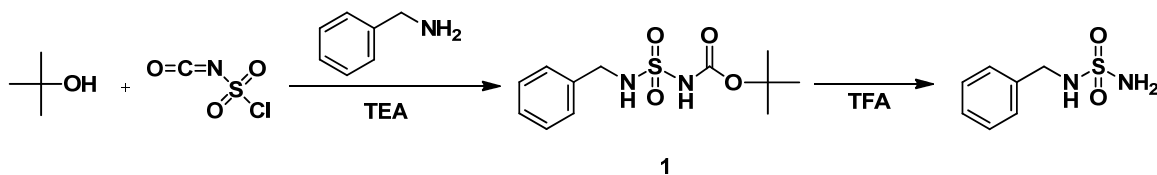
products (Scheme 2). Along this line, in this investigation, the kinetics of benzylsulfamide preparation as a degradation product of precursor **1** was studied.

In this work isoconversional and master-plot methods from non isothermal thermogravimetric data are used. The model-free method is used to simulate the isothermal experiments. Theoretical calculations of the activation energy were also done using HyperChem 7.0.

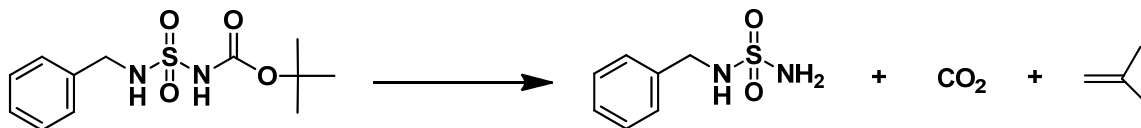
The purpose of this study is to perform an analysis of thermolysis of *N*-(benzyl)-*N'*-(*tert*-butoxycarbonyl) sulfamide to yield benzylsulfamide to obtain a representation of reaction data. The information obtained will help to determine the optimal conditions to prepare benzylsulfamide.

2. Experimental

Initially the precursor **1**, the *N*-(benzyl)-*N'*-(*tert*-butoxycarbonyl) sulfamide, was synthesized following the standard procedure [11]. It was obtained in one-pot synthesis from chlorosulfonyl isocyanate, *tert*butanol and benzylamine, in presence of triethylamine in a solution of dried CH₂Cl₂. After that, the thermo degradation of precursor **1** was investigated by means of dynamic thermogravimetry (TGA) using a Shimadzu TGA-50 equipment under atmospheric pressure. The method of multiple heating rate programs (multiple temperature programs) was used as recommended by the ICTAC Kinetics Committee [13]. Studies were carried out at constant heating rates between 0.2 to 10 °C/min in He stream (50 mL/min) flowing onto the cylindrical sample holder. As in all experiments using the method of multiple heating rate programs, one first stage by heating at 20 °C/min up to 105 °C and then a second stage at the selected heating rate were performed.



Scheme 1



Scheme 2

Isothermal experiments were carried out at 115, 120 and 130 °C. In isothermal experiments, the heating rate between room T and the selected T was 20 °C/min (sample: 10 mg).

The melting point of the precursor 1 was determined using an equipment of Differential Scanning Calorimeter model DSC 50 Shimadzu. For this, a sample of 5 mg, a sealed aluminum sample holder, N₂ flow (100 mL/min) and a heating rate 5 °C/min were used.

3. Kinetic analysis

Several heterogeneous solid-gas reactions, such as the diesel soot oxidation [14-16], degradation of polymeric materials [17], synthesis and thermal behavior of new nitro compounds [18] and decomposition of colorants [19], can be kinetically evaluated by means of thermogravimetric methods.

Experimental data for the kinetic analysis of reactions can be obtained by means of dynamic thermogravimetry at constant heating rate. Under such conditions, the reaction rate is usually expressed by the general equation:

$$d\alpha/dt = A f(\alpha) \exp(-E_a/RT) \quad (1)$$

where α is the conversion, A is the pre-exponential factor, E_a is the activation energy, $f(\alpha)$ is the differential conversion function, and R is the gas constant. Equation (1) presumes that the kinetic rate is the product of a function of temperature $A \exp(-E_a/RT)$ by a function of the extent of conversion noted $f(\alpha)$.

If experiments are performed at constant heating rate ($dT = \beta dt$), equation (1) can be expressed like a derivative as a function of the temperature

$$d\alpha/dT = (A/\beta) f(\alpha) \exp(-E_a/RT) \quad (2)$$

Introduction of the explicit value of the heating rate reduces the applicability of equation (1) to processes in which the sample temperature does not deviate significantly from the reference temperature.

Integration of kinetic equation (2) leads to the following equation

$$g(\alpha) = \int d\alpha / f(\alpha) = (A/\beta) \int \exp(-E_a/RT) dT = (A E_a/R \beta) \int \exp(-x)/x^2 \cdot dx = (A E_a/R \beta) p(x) \quad (3)$$

where $g(\alpha)$ is the integral form of the reaction model, and $p(x)$ is the temperature integral, for $x = E_a/RT$.

3.1. Isoconversional method

Isoconversional methods permit the effective activation energy of a process to be estimated as a function of the conversion without the assumption of the reaction model $f(\alpha)$. Such kinetic analysis requires a series of thermoanalytical curves, recorded at several constant heating rates. In this work, the approximation of Kissinger-Akahira-Sunose method is used.

$$\ln(\beta/T^2) = \ln(AR/E_a g(\alpha)) - E_a/RT \quad (4)$$

Thus, for a certain conversion (α), the plot of $\ln(\beta/T^2)$ versus $1/T$ obtained from thermogravimetric curves and recorded at different heating rates should be a straight line whose slope can be used to evaluate the activation energy.

3.2. Master-plot method

The application of this method usually leads to the selection of the appropriate conversion model for the solid-state reaction investigated. Mathematically, the use of this master-plot method for kinetic data recorded under non isothermal conditions is described as follows.

By using a reference at point $\alpha = 0.5$ and according to equation (3), the following equation is obtained:

$$g(0.5) = (A E_a/\beta R) p(x_{0.5}) \quad (5)$$

where $x_{0.5} = E_a/RT_{0.5}$, and $T_{0.5}$ is the temperature required to attain 50% conversion. When equation (3) is divided by equation (5), the equation (6) is deduced:

$$g(\alpha)/g(0.5) = p(x)/p(x_{0.5}) \quad (6)$$

The ratio $g(\alpha)/g(0.5)$ is calculated and plotted as a function of " α " for all functions $g(\alpha)$.

The most commonly used reaction models for solid-state processes were cited by Vlaev [20] and Vyazovkin [21] and are listed in Table 1.

Both the conversion-temperature profile (α -T) and the value of E_a for the process should be known in advance to draw the experimental master plots of $p(x)/p(x_{0.5})$ versus " α " from experimental data obtained at a given heating rate. Thus, equation 6 indicates that, for a given α , the experimental value of $p(x)/p(x_{0.5})$ and theoretically calculated values of $g(\alpha)/g(0.5)$ are equivalent when an appropriate conversion model is used.

Table 1. Conversion model functions usually employed for solid-state reactions.

Code	Reaction Model	$f(\alpha)$	$g(\alpha)$
R1 A1	Chemical reaction (first order) Nucleation and growth (Avrami-Erofeev equation)	$1-\alpha$	$-\ln(1-\alpha)$
A1.5	Nucleation and growth (Avrami-Erofeev equation)	$1.5(1-\alpha)(-\ln(1-\alpha))^{0.5/1.5}$	$(-\ln(1-\alpha))^{1/1.5}$
A2	Nucleation and growth (Avrami-Erofeev equation)	$2(1-\alpha)(-\ln(1-\alpha))^{1/2}$	$(-\ln(1-\alpha))^{1/2}$
A3	Nucleation and growth (Avrami-Erofeev equation)	$3(1-\alpha)(-\ln(1-\alpha))^{2/3}$	$(-\ln(1-\alpha))^{1/3}$
P1	Phase boundary controlled reaction (contracting linear)	1	α
P2	Phase boundary controlled reaction (contracting area)	$2(1-\alpha)^{1/2}$	$(1-(1-\alpha)^{1/2})$
P3	Phase boundary controlled reaction (contracting volume)	$3(1-\alpha)^{2/3}$	$(1-(1-\alpha)^{1/3})$

4. Theoretical calculation of the activation energy

Geometry optimizations were conducted for the reactant and the products showed in Scheme 1, in order to find the most stable conformation for each molecule. The conformational search module included in the HyperChem 7.0 package was employed [22], and the usage directed scheme to sample the initial conformations was applied. The initial structures were modified by varying geometric parameters (dihedral angles) and each modified structure was optimized to get the energy minimized conformations. After that, these conformations were compared and the conformation was accepted if it is new and it satisfies the energy criterion (lower energy than the one previously found). The process was repeated until the lowest energy value was found for each molecule. The calculations were performed at PM3 level and default parameters provided by the HyperChem 7.0 software [22] were employed.

Once the most stable conformations were determined for the reactant and the products, the transition states were detected using the linear synchronous transit approach [22]. This method allowed us to calculate transition states by defining how the atoms are rearranged through the transition state. Based on previous studies [12], it was proposed that the precursor **1** yielded benzylsulfamide, carbon dioxide and 2-methyl propene in the course of an intra-molecular elimination reaction. The interpolation parameter λ as 0.5 was defined since its value ranges from 0 for the reactant state to 1 for the product state. Reactant and product atoms were matched, and a starting point for the search was interpolated from the initial and final configurations. From this calculation, transition state energy was calculated. Results are given in Results and discussion section.

5. Results and discussion

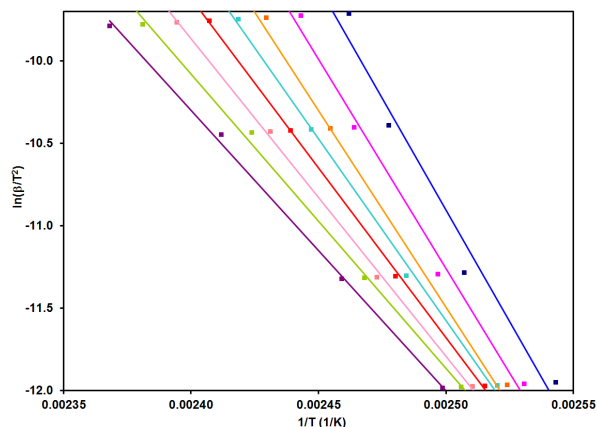
5.1. Isoconversional method

The thermoanalytical curves (weight loss versus temperature) obtained at constant heating rate were transformed into conversion-temperature curves. According to the KAS method, the activation energy was obtained from the slope of the resulting linear adjustment after plotting $\ln(\beta/T^2)$ versus $1/T$ at several constant conversion α . Figure 1 shows the linear relationships obtained for thermolysis of *N*-(benzyl)-*N'*-(*tert*-butoxycarbonyl) sulfamide.

Results derived from KAS method in terms of the activation energy as function of the conversion are listed in Table 2. The activation energy calculated by this method varies significantly with the degree of advance of the reaction.

Table 2. Activation energy as a function of conversion for thermolysis of *N*-(benzyl)-*N'*-(*tert*-butoxycarbonyl) sulfamide.

α	E_a (kJ/mol)	r^2
0.1	225.2	0.9712
0.2	210.9	0.9895
0.3	198.2	0.9830
0.4	183.3	0.9969
0.5	171.1	0.9993
0.6	160.2	0.9988
0.7	148.4	0.9976
0.8	141.3	0.9984

**Figure 1.** Isoconversional method, $\alpha = 0.1$, $\alpha = 0.2$, $\alpha = 0.3$, $\alpha = 0.4$, $\alpha = 0.5$, $\alpha = 0.6$, $\alpha = 0.7$, $\alpha = 0.8$.

5.2. Theoretical estimation of activation energy

Since the activation energy calculated by the KAS method is modified with the degree of conversion, a theoretical estimation of activation energy was performed as complement. Table 3 summarizes the results obtained for the calculation of the energies of reactant, products and transition state. From this data, the activation energy 267 kJ/mol was estimated as the difference between the energy value of the transition state and the reactant.

Table 3. Calculated energies (kJ/mol) for reactants, products and transition state. Energy changes are included in columns 4.

E reactants	E transition state	E products	Activation energy
-326271	-326003	-326227	267

5.3. Determination of the conversion model

The knowledge of α as a function of temperature and the value of the activation energy are essential in order to calculate the experimental master plot of $p(x)/p(x_{0.5})$ against α from experimental data obtained under a linear heating rate. The activation energy estimated by theoretical calculation from Transition State Theory (267 kJ/mol) is used to calculate the master plot. Figure 2 and 3 shows the theoretical master plots corresponding to the $g(\alpha)/g(0.5)$ functions and experimental master plot for all heating rates (0.2-10.0 °C/min).

The comparison of experimental master plots with the theoretical ones revealed that the kinetic process for precursor **1** degradation was most probably described by the Avrami-Erofeev model, with the $1.5 < m < 2.0$ (Figure 2) for heating rates between 0.2 and 0.5 °C/min. For very high heating rates, between 5 and 10 °C/min, experimental results fit with a first-order reaction.

To interpret that behavior difference, conversion (α) results are presented here as function of temperature. Figure 4 shows that there is a shift toward higher temperature when the experiment is carried out at higher heating rate.

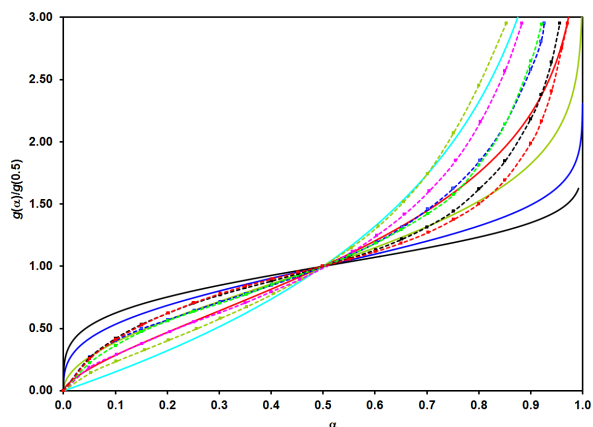


Figure 2. Master plots of theoretical $g(\alpha)/g(0.5)$ vs. α for the conversion models. \blacksquare 10 °C/min \blacksquare 5 °C/min \blacksquare 2 °C/min \blacksquare 1 °C/min \blacksquare 0.5 °C/min \blacksquare 0.2 °C/min, — A1, R1, $(-\ln(1-\alpha))$, — A1.5, $((-\ln(1-\alpha))^{1/1.5})$, — A2, $((-\ln(1-\alpha))^{1/2})$, — A3, $((-\ln(1-\alpha))^{1/3})$, — A4, $((-\ln(1-\alpha))^{1/4})$.

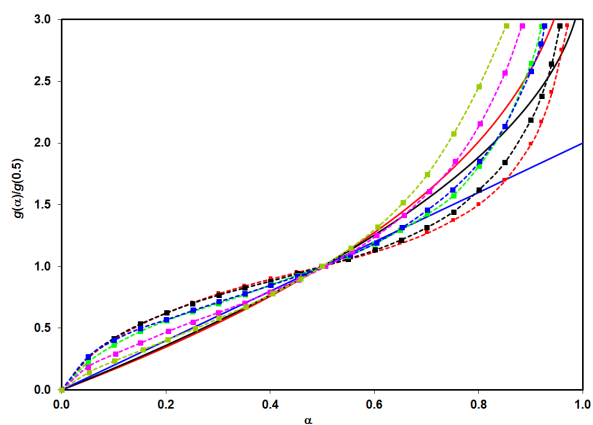


Figure 3. Master plots of theoretical $g(\alpha)/g(0.5)$ vs. α for the conversion models. \blacksquare 10 °C/min \blacksquare 5 °C/min \blacksquare 2 °C/min \blacksquare 1 °C/min \blacksquare 0.5 °C/min \blacksquare 0.2 °C/min, — P3, $(1-(1-\alpha)^{1/3})$, — P2, $(1-(1-\alpha)^{1/2})$, — P1, (α) .

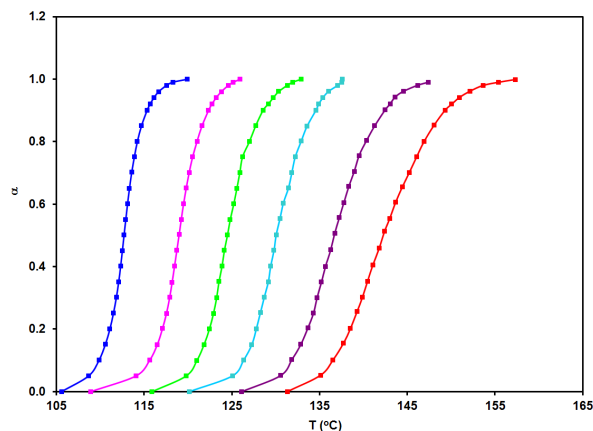


Figure 4. Conversion vs. temperature for different heating rates. \blacksquare 0.2 °C/min, \blacksquare 0.5 °C/min, \blacksquare 1.0 °C/min, \blacksquare 2.0 °C/min, \blacksquare 5.0 °C/min, \blacksquare 10.0 °C/min.

Thus, for example, for a heating rate of 0.2 °C/min, the experiments occurred between 105 and 120 °C, instead, for a heating rate of 10 °C/min, the reaction occurred between 131

and 157 °C. The DSC diagram of the precursor **1** (Figure 5) showed that the melting point is 133.5 °C.

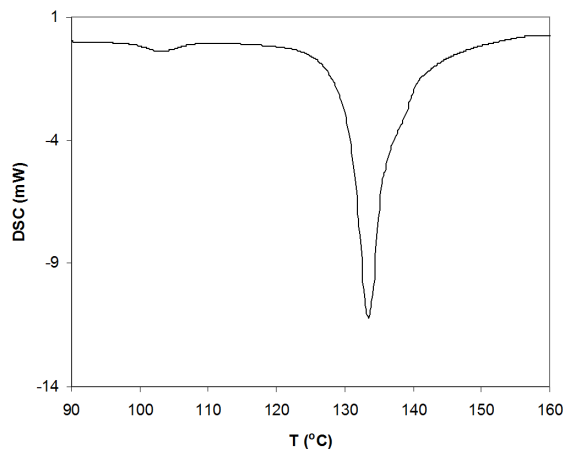


Figure 5. DSC of *N*-(benzyl)-*N'*-(tert-butoxycarbonyl) sulfamide.

In the experiment performed with a heating rate of 0.2 °C/min, the precursor **1** was found in solid state, instead, for the experiment with a heating rate of 10 °C/min, it was found in liquid state from the reaction beginning. These results explain why when the heating rate is low; the reaction can be interpreted with a reaction model in solid state (Avrami-Erofeev model). On the other hand, for the highest heating rate, the precursor **1** was found as a liquid, and the reaction can be modeled as a first-order reaction.

5.4. Simulation of isothermal experiments. Model-free method

Isothermal experiments performed at 115, 120, and 130 °C were simulated using the model-free method proposed by Vyazovkin [23] and results of this simulation are shown in Figure 6. The activation energy theoretically calculated was used to simulate isothermal experiments (267 kJ/mol). The DSC diagram of the precursor **1** (Figure 5) showed that at 120 °C the melting has already started. Results show that the better adjustment is observed for experiments of higher temperature (120 and 130 °C) where the precursor is found initially in liquid state. The experiment that occurs at the beginning with the precursor in solid state does not present so precise adjustment.

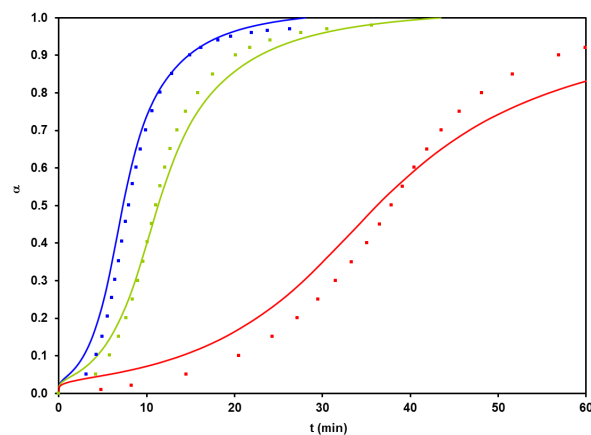


Figure 6. Isothermal experiment at 115, 120, and 130 °C. Model-free method. Theoretical — 130 °C, — 120 °C, — 115 °C; Experimental, \blacksquare — 130 °C, \blacksquare — 120 °C, \blacksquare — 115 °C.

6. Conclusion

The kinetics of the thermolysis of *N*-(benzyl)-*N'*-(*tert*-butoxycarbonyl) Sulfamide was accurately determined from a series of thermoanalytical experiments at differing constant heating rates. As the activation energy calculated by the isoconversional KAS method varies substantially with the conversion, the activation energy was estimated theoretically. The DSC diagram of the precursor shows that the melting at 120 °C is already begun. In experiments carried out with low heating rate (final $T < 120^{\circ}\text{C}$), the precursor **1** was found in solid state and in experiments performed at higher heating rate (final $T > 135^{\circ}\text{C}$), it was found in liquid state during the reaction that yielded benzylsulfamide. Master Plot method showed that at low heating rate the reaction fits with a model of solid-gas state type (Avrami-Erofeev). In these experiments, the temperature range was lower than the melting point of the precursor **1** (133.5 °C) and the reaction occurred in solid state. When the heating rate is high, experimental data are fitted with a first-order reaction and in these experiments, the reaction occurs in liquid state.

To predict the time required for the reaction to completely occurs in an isothermal system, the so called Model-free method was used. Experimental curves obtained with this method fit well with the theoretical ones for experiments performed with $T > 120^{\circ}\text{C}$. From the experiments we conclude that the best conditions for the preparation of benzylsulfamide can be realized at temperatures higher than 120 °C during a very short time (40 min).

Acknowledgements

Ileana Daniela Lick and Luciana Gavernet are researchers from Consejo Nacional de Investigaciones Cientificas y Tecnicas de la Republica Argentina (CONICET). This research was supported in part through grants from Agencia de Promocion Cientificay Tecnologica, CONICET, and Universidad Nacional de La Plata, Argentina.

References

- [1]. Backbro, K.; Lowgren, S.; Osterlund, K.; Atepo, J.; Unge, T.; Hulten, J.; Bonham, N. M.; Schaal, W.; Hallberg, A. *J. Med. Chem.* **1997**, *40*, 898-902.
- [2]. Hulten, J.; Bonham, N. M.; Nillroth, U.; Hansson, T.; Zuccarello, G.; Bouzide, A.; Aqvist, J.; Classon, B.; Danielson, U. H.; Karlen, A.; Kvarnstrom, I.; Samuelsson, B.; Hallberg, A. *J. Med. Chem.* **1997**, *40*, 885-897.
- [3]. Castro, J. L.; BakerGiublin, A. R.; Hobbs, S. C.; Jenkins, M. R.; Russell, M. G.; Beer, M. S.; Stanton, J. A.; Scholey, K.; Hargreaves, R. J. *J. Med. Chem.* **1994**, *37*, 3023-3032.
- [4]. Acheson, R. M.; Bite, M. G.; Kemp, J. E. *J. Med. Chem.* **1981**, *24*, 1300-1304.
- [5]. Dougherty, J. M.; Probs, D. A.; Robinson, R. E.; Moore, J. D.; Klein, T. A.; Snelgrove, K. A.; Hanson, P. R. *Tetrahedron* **2000**, *56*, 9781-9790.
- [6]. Abbate, F.; Supuran, C. T.; Scozzafava, A.; Orioli, P.; Stubbs, M. T.; Klebe, G. *J. Med. Chem.* **2002**, *45*, 3583-3587.
- [7]. Winum, J. Y.; Innocenti, A.; Nasr, J.; Montero, J. L.; Scozzafava, A.; Vullo, D.; Supuran, C. T. *Bioorg. Med. Chem. Lett.* **2005**, *15*, 2353-2358.
- [8]. Casini, A.; Winum, J. L.; Montero, J. L.; Scozzafava, A.; Supuran, C. T. *Bioorg. Med. Chem. Lett.* **2003**, *13*, 837-840.
- [9]. Winum, J. Y.; Cecchi, A.; Montero, J. L.; Innocenti, A.; Scozzafava, A.; Supuran, C. T. *Bioorg. Med. Chem. Lett.* **2005**, *15*, 3302-30306.
- [10]. Maryanoff, B. E.; McComsey, D. F.; Costanzo, M. J.; Hochman, C.; Smith-Swintosky, V.; Shank, R. P. *J. Med. Chem.* **2005**, *48*, 1941-1947.
- [11]. Gavernet, L.; Barrios, I.; Sella-Craverro, M.; Bruno-Blanch, L. E. *Bioorg. Med. Chem.* **2007**, *15*, 5604-5614.
- [12]. Lick, I. D.; Gavernet, L.; Bruno-Blanch, L. E.; Ponzi, E. N. *Thermochim. Acta* **2010**, *501*, 30-34.
- [13]. Vyazovkin, S.; Burnham, A. K.; Criado, J. M.; Perez-Maqueda, L. A.; Popescu, C.; Sbirrazzuoli, N. *Thermochim. Acta* **2011**, *520*, 1-19.
- [14]. Lopez-Fonseca, R.; Landa, I.; Elizundia, U.; Gutierrez-Ortiz, M. A.; Gonzalez-Velasco, J. R. *Chem. Eng. J.* **2007**, *129*, 41-49.
- [15]. Lopez-Fonseca, R.; Elizundia, U.; Landa, I.; Gutierrez-Ortiz, M. A.; Gonzalez-Velasco, J. R. *Appl. Catal. B* **2005**, *61*, 150-158.
- [16]. Bokova, M. N.; Decarne, C.; Abi-Aad, E.; Pryakhin, A. N.; Lunin, V. V.; Aboukais, A. *Thermochim. Acta* **2005**, *428*, 165-171.
- [17]. Vrandecic, N. S.; Erceg, M.; Jakic, M.; Klaric, I. *Thermochim. Acta* **2010**, *498*, 71-80.
- [18]. Liu, L.; Jian, Y.; Li, Z.; Li, C. *Thermochim. Acta* **2012**, *54*, 125-130.
- [19]. Rotaru, A.; Moa, A.; Rotaru, P.; Segal, E. *J. Therm. Anal. Cal.* **2009**, *95*, 161-166.
- [20]. Vlaev, L. T.; Markovska, I. G.; Lyubchev, L. A. *Thermochim. Acta* **2003**, *406*, 1-7.
- [21]. Vyazovkin, S.; Wight, C. A. *Thermochim. Acta* **1999**, *340-341*, 53-68.
- [22]. HyperChem(TM) Professional 7. 51., Hypercube, Inc.; 1115 NW 4th Street, Gainesville, Florida 32601, USA.
- [23]. Vyazovkin, S. *Int. J. Chem. Kinet.* **1996**, *28*, 95-101.